# A COMSOL Model of Damage Evolution Due to High Energy Laser Irradiation of Partially Absorptive Materials

**J.J. Radice*, P.J. Joyce, A.C. Tresansky, R.J.Watkins**
Mechanical Engineering Department, United States Naval Academy
*Corresponding author: 590 Holloway Road, Annapolis, MD, 21402. radice@usna.edu

**Abstract:** In this paper we present a numerical model of the transient heat transfer and thermochemical damage evolution in an IR opaque material using COMSOL Multiphysics. The model is applied to a carbon black loaded PMMA (polymethyl-methacrylate), using material properties available in the literature supplemented with experiments. This variant of PMMA was chosen because it is homogeneous, isotropic, and the decomposition from solid to gas is relatively straightforward to characterize. The incident high energy laser beam is modeled as a Gaussian heat flux. The beam parameters used for this study are selected to mimic that of a Nd:YAG high energy laser with a wavelength of 1070nm, an output power of 110W, and a spot size with a 5.5mm beam diameter. At this wavelength, NIRS/FTIR experiments demonstrate that PMMA absorbs slightly more than half of the incident laser energy. PMMA was experimentally observed to vaporize from 310°C to 475°C via differential scanning calorimetry. The temperature range and endothermic phase change from solid to gas is incorporated in the COMSOL model. Rather than use an adaptive mesh , material removal (or ablation) is captured using temperature and phase dependent material properties. The model captures vaporization material removal by appropriately varying the thermal conductivity and density of the PMMA at the vaporization temperature. The model results are compared to experiments on carbon-laden PMMA.

**Keywords:** Heat Transfer, Phase Change, High Energy Laser, Material Damage, Ablation

## 1. Introduction

Composite materials have shown a marked increase in their use in aerospace and military applications in recent years. Concurrent maturation of the technology in near Infrared High Energy Lasers (HEL) has shown promise for their use in directed energy weaponry. The intersection of these two technologies will likely occur in the near future. A numerical method for predicting the resultant transient temperature field from the interaction of a high energy laser and structural materials could aid in the prediction of damage caused by the HEL.

In the present work, we propose a numerical model for the transient temperature field and damage evolution resulting from high energy near infrared laser irradiation incident on a monolithic polymeric material. The matrix phase of many common aerospace composite materials are made of polymeric materials, therefore modeling pure polymer ablation provides an avenue to begin capturing composite material response to such insults. The investigation begins with a transient heat transfer model of a linearly ablating polymer. For the present purposes, we have chosen to model polymethyl-methacrylate, or PMMA, in the COMSOL Multiphysics environment. The model developed here incorporates material ablation and the concomitant simulated change of boundary conditions/damage evolution. We have accomplished this by simulating phase change to account for the latent heat of vaporization and by artificially varying material properties to simulate the moving boundary condition of the incident laser energy boring through the material.

## 2. Background

Many studies have been published on the laser ablation of polymers and polymeric materials. Cozzens studied the infrared ablation of polymers using a 10.6μm laser and related ablation energy to irradiance as well as investigating the method of ablation [1]. Lloyd and Myers studied the use of ablative polymeric materials for near IR (1.06μm) High Energy Laser beam diagnostics, and suggested the use of

linearly ablating polymers like PMMA for this application [2]. Crane and Brown also studied laser ablation in multiple composite materials and suggested damage mechanisms [3]. Numerous studies have been conducted on the use of high energy lasers for drilling or machining composites [4-8]. Further studies have also been conducted into modeling laser effects, and the resulting temperature field using finite element and finite difference methods [9-12]. When applied to the near-IR HEL case, these studies fall short in one of two areas. They are either focused on the use of $CO_2$ lasers (which laze at a wavelength 10 times longer than near-IR Nd:YAG lasers) or they deal with solely industrial machining contexts. These different wavelengths and irradiance levels produce different results when irradiating composite or even simple polymer materials. The need for more research has been suggested dealing with the irradiance of polymers and composites in the 100-600 W/cm$^2$ irradiance range [13] which is with readily available (or soon to be available) solid state Nd:YAG lasers [14].

In the present work, we have chosen PMMA as an example material to validate our COMSOL model because of its recommendation as a linearly ablating polymer [15], it's extensive use in this context, and to facilitate experimental verification. Linear ablation in the present context means that the polymer unzips into monomer fragments ejected as gas, and the ablation rate demonstrates a highly linear correlation to incident power. We have further chosen to model and use PMMA loaded with carbon black. This is because small concentrations of carbon black (<0.1% by weight) lead to near 0% transmittance of the 1.07μm wavelength. It has also been demonstrated that at this wavelength approximately 50% is reflected but ~0% is transmitted which allow us to treat PMMA as a surface absorber with relatively high reflectivity [16]. For longer wavelength IR light PMMA reacts photothermally [16], whereas for short wavelength UV excimer laser light, PMMA reacts photochemically [17]. The photothermal effect suggests that the laser photons do not possess sufficient energy to sever the chemical polymer bonds in the plastic, and therefore multiple photons must be absorbed and transformed into heat via vibration of the molecule before these polymer bonds are severed [18]. Finite element models and studies of these two effects on PMMA suggest pit formation and the high velocity ejection of monomer gases upon irradiation from either source. Because the material reacts to the laser photothermally, it is assumed here that the laser can be modeled as a Gaussian heat flux at the irradiation surface. The irradiation surface will, in turn, proceed through the thickness due to ablation/material removal as long as the focal length is great enough that the beam radius is independent of the through thickness position [19]. Therefore, the removal of material can be modeled as vaporization caused by temperature rise from the laser induced heat flux.

## 3. COMSOL Model

### 3.1 Physics

To capture the laser damage propagation through the representative material, a COMSOL Transient Heat Transfer model was created. This model includes four primary heat transfer mechanisms: conduction, convection, radiation , and sublimation phase change from solid to vapor. The initial conditions of the domain were the default room temperature.

### 3.2 Geometry and boundary conditions

The overall geometry of the laser incidence problem considered here is included in Figure 1:

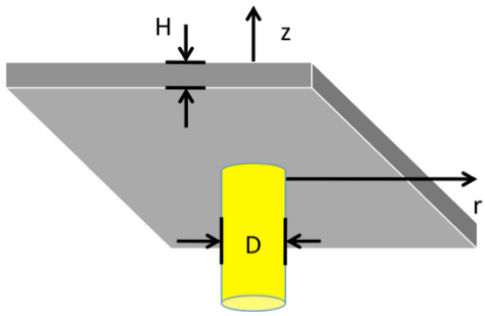


**Figure 1**. Problem Definition

In contrast with the aerospace grade composite materials that are the ultimate goal of this research program, the material considered here is isotropic, and thus has the same physical, mechanical, and thermal properties in all directions. In practice, the laser emanates as

"nearly Gaussian" and is further distorted as it propagates through a chaotic atmosphere until it reaches a target. There are significant efforts underway in the literature to quantify these effects on the beam profile, but for the present study, the beam is assumed to be an axisymmetric Gaussian profile. The isotropy of the sample and the assumed axisymmetry of the beam allow for the use of an axisymmetric domain for the COMSOL model. As is well known, this approach streamlines computation and allows for a higher fidelity mesh.

Axisymmetry provides one boundary condition; three more are required for an asymmetric model. On the incident face, the Gaussian laser is modeled as an applied heat flux matching the laser geometric parameters as discussed below. The laser dimensions are relatively small compared to the dimensions of the structure of interest, therefore an open boundary condition is applied opposite the edge of axial symmetry. Finally, the face opposite the laser incidence is cooled both convectively and conductively. The axisymmetric model domain is shown in Figure 2:

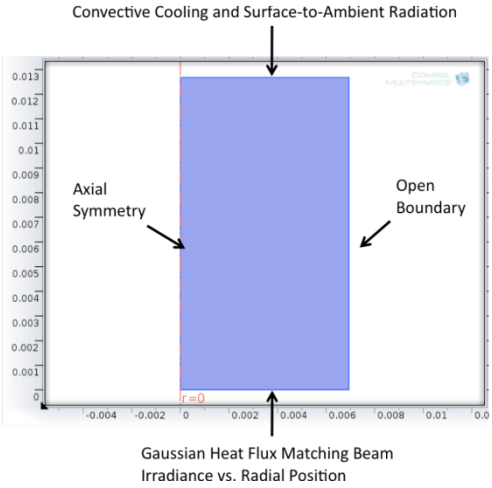


**Figure 2**. Axisymmetric Problem Domain

### 3.3 Laser Modeling

At the United States Naval Academy Directed Energy Laboratory, we have a 110W, 1070nm laser with a beam diameter of 5.45mm with an approximately Gaussian profile ($M^2$=1.07). The expression for the Irradiance of a Gaussian profile is expressed as follows:

$$I(r) = I_0 e^{-8\frac{r^2}{D^2}} \quad (1)$$

where $r$ is the radial position, $I_0$ is the peak irradiance at the beam centerline, $D$ is the beam diameter, and the irradiance has units of power per unit area.

In the context of a Gaussian profile, the total laser power corresponds to the spatial integration of equation (1) over the infinite plane perpendicular to the beam propagation direction. However, for Gaussian profiles, the majority of the energy is concentrated near the center axis of the propagating beam. At 2.5 beam diameters, the irradiance has decayed to 0.00037% of the peak irradiance and a truncation of the domain to 2.5 beam diameters captures 99.9996% of the energy. As such, the profile defined in (1) is implemented in the COMSOL model but truncated to zero beyond 2.5 beam diameters. The Gaussian profile for a beam with the USNA beam specifications is shown in Figure 3:

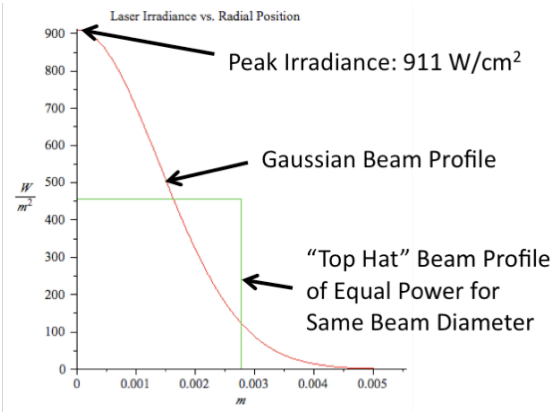


**Figure 3**. Gaussian Beam Laser Irradiance vs. Radial Position

It can be seen in Figure 3 that a spatially constant power distribution (or a "top-hat" beam profile) results in a peak irradiance that is exactly half the peak power of the Gaussian profile from equation (1). The reason that Figure 3 has been presented here is to highlight the fact that the peak irradiance is near the centerline of the beam and is where one should expect to see the beam damage advance the most quickly.

### 3.4 Modeling Phase Change

Although there exists a functional two phase heat transfer module within COMSOL, this approach is eschewed in favor of a single phase model in which the phase transition at a given location from solid to gas is controlled explicitly. The governing equation for the transient heat transfer module is given as follows:

$$\rho C_p \frac{\partial T}{\partial t} - k\nabla^2 T = g \qquad (2)$$

where $\rho$ is the density, $C_p$ is the specific heat, k is the thermal conductivity, $g$ is a distributed heat generation term, and $T$ is the temperature field as a function of space and time.

Prior to a sublimation phase change, all thermal energy transferred to a material causes the temperature to increase. However, during a phase transition, the temperature tends to stop changing while the material absorbs latent energy to break the various molecular bonds that keep it in the current state.

There are two ways to capture this effect in equation (2). The first way would be to be an endothermic heat sink term that is active over the temperature range of the phase change and absorbs the latent heat of transformation. This method is a challenge, as the quantity of energy absorbed at each location must be tracked to determine if phase transition has been completed. The more preferable method is the use of variable specific heats ($C_p$) that become significantly larger over the temperature range of the phase change. By this approach, the temperature change will tend to stop over the duration of the phase change as is seen in the experiment.

To this end, proceeding as suggested in [20], we define a parameter to track the progress of the material over the phase change temperature range:

$$h(T) = (T - T_1)H(T - T_1)H(T_2 - T) + H(T - T_2) \qquad (3)$$

where $h$ is the phase transformation tracking parameter that is zero when the PMMA is solid and 1 when the PMMA vaporizes and departs. $T_1$ is the temperature where the phase change begins, $T_2$ is the temperature where the phase change ends, and $H$ is the Heaviside Step Function.

It is convenient that expression (3) corresponds closely to COMSOL's smoothed Heaviside function:

$$h(T) = flc2hs(T - T_1, T_2 - T_1) \qquad (4)$$

where expression (4) is the expression for the phase parameter as-implemented in the COMSOL model presented here.

Again, proceeding as in [20], we define a parameter for the first derivative of the phase change as follows:

$$d(T) = \frac{dh}{dT} \qquad (5)$$

As solid materials are heated from ambient temperature with the laser, they reach a temperature range where the material undergoes an endothermic reaction whilst the phase is changing from solid (very briefly through liquid) to vapor. The quantity of energy absorbed during this phase change is referred to as the latent heat. To accommodate the latent heat of phase change, the specific heat is suitably modified as follows:

$$C_p(T) = C_{ps} + d(T)\Delta_h \qquad (6)$$

Where $\Delta_h$ is the latent heat of vaporization and has units of energy per mass. It can be seen as in [21] that the form of (6), when integrated over the temperature range of phase transition accounts for the total endothermic energy of material transformation.

### 3.5 Damage Progression Modeling

During laser burn-through experiment, a high velocity jet of vapor and debris can be seen emanating from the laser damage site. This corresponds to the vaporization of material and a hole evolving through the thickness of the sample. As this material departs, it carries it's thermal energy with it and allows the laser to strike the newly exposed surface that is revealed as the hole progresses.

These two highly relevant effects are interesting challenges to implement in the model. Several efforts in the literature have attempted to do so with dynamic meshing. However, with an eye towards transitioning to the damage evolution through anisotropic sandwich structured materials, dynamic meshing is seen as being computationally expensive. The present work

offers three simply implemented numerical techniques to account for these effects.

First, to account for the removal of thermal energy, once the phase parameter (4) reaches unity for a given location, the density and specific heat of affected material are transitioned to that of air/vaporous PMMA. With the understanding that the thermal energy is the product of the density, the specific heat, and the temperature, by "nulling out" the density and specific heat we are mathematically removing an amount of energy from the system corresponding to the mass and heat flow associated with the exhaust jet without the complexity of modeling this highly intricate energy removal mechanism. Again, this is a purely mathematical approach but it is well grounded in a physical meaning and is a first order engineering approximation for the quantity of energy removed by the exhaust gases .

Accounting for the evolution of the hole and the transition of the laser damage to the newly exposed surface are also interesting and challenging phenomena to capture. In the present study, the laser energy is applied as a heat flux with Gaussian spatial profile. However, this heat flux is applied at a static location, namely the domain boundary shown in Figure 2. To computationally apply the laser heat flux to the newly exposed hole surface, we propose to mathematically elevate the thermal conductivity in the beam propagation direction ($z$) to several orders of magnitude higher than the parent material. Furthermore, to mandate that the laser power flows and the damage progresses predominantly in the direction of beam propagation, the thermal conductivity perpendicular to the beam direction ($r$) is reduced to several orders of magnitude less than the parent material.

In concert, the transition of the density/specific heat to that of air, the beam-direction thermal conductivity becoming extremely large, and the radial conductivity becoming extremely small effectively eliminates all material between the boundary of the model and the laser damage front. As such, one can also use the phase parameter (4) as the variable with which to track the hole progression; anywhere $h$ is equal to unity is a location where there is no longer material.

### 3.6 Model Parameters

The majority of physical and thermal properties of PMMA such as the density, thermal conductivity, and specific heat are well canvassed in the literature. The experiments with which this model is to be compared use a commercially available PMMA material with the trade name Acrylite GP. The properties that are less well known pertain to the latent heat of phase change ($\Delta_h$) and the reflectance of the PMMA to the 1070nm laser light.

Determination of the latent heat of phase change from solid to vapor is done with the use of a differential scanning calorimeter (DSC). The DSC takes a sample with a known mass through a temperature excursion from room temperature to the upper extreme of the equipment, measuring the thermal power absorbed/released by the sample. From this plot, one is able to observe the phase change endotherm/exotherm for a given material and quantify the heat associated with the phase change. A representative DSC can for Acrylite GP is presented in Figure 4.

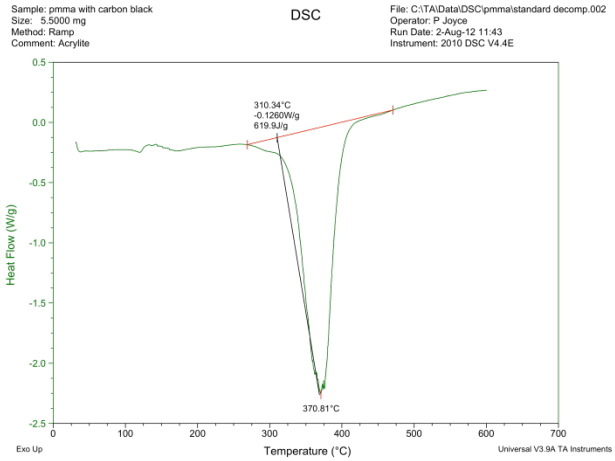


**Figure 4**. DSC of Acrylite GP PMMA

The trough is the phase change endotherm from solid to vapor. The temperature range of this transformation is determinable from where the trough begins and ends. The area of the trough is the latent heat of phase change.

As cited in the literature, the reflectivity of Acrylite GP to the 1070nm laser can be extracted from a Near-Infrared Reflective Spectroscope, or NIRS. Lloyd performed this experiment on the same material and determined that the Acrylite GP reflects 45% of the incident energy at 1070nm [16]. In the present model, this fact is used to effectively reduce the power that is applied to/absorbed by the domain to 55% power power absorbed by the PMMA material.

## 4. Simulation Results

The material properties, laser parameters, heat transfer coefficients, and geometric parameters used in the model are presented in the Appendix in Table 1. After running the laser ablation experiment in the USNA Directed Energy Laboratory, it was observed that a nominally 0.25in. thick PMMA sample burns through in approximately two seconds and a nominally 0.5in. thick PMMA sample burns through in roughly twice that. To compare to the experimental measurements described below, we have chosen to model the first two seconds of a laser ablation experiment through the thinner of these two samples.

The progression of the hole/phase change for various time is shown in Figure 5:

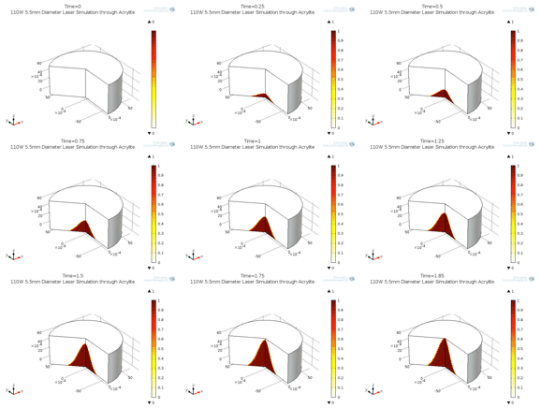

**Figure 5**. Simulated Hole Progression vs. Time

Figure 5 shows the simulated progression of the phase change hole through the thickness sample in approximately 1.85s. In the interest of quantitative comparison to the experimental results, the centerline hole depth as a function of time was extracted and plotted in Figure 6.

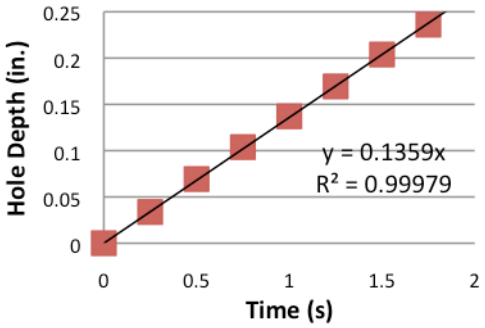


**Figure 6**. Simulated Hole Depth vs. Time

Figure 6 suggests that the hole depth evolves approximately linearly with respect to time. The hole progresses at a rate of approximately 0.136in/s. At the end of the simulation, the diameter of the drilled hole on the boundary of laser incidence was investigated and determined to be 0.291in.

## 5. Experimental Comparison

As stated previously, laser burn-through experiments were run in the United States Naval Academy Directed Energy Laboratory. These were performed with the beam parameters defined in Table 1 and used in the above simulation. The material was the PMMA Acrylite GP with a measured thickness of 0.248 in. The approach to these experiments was to irradiate a given location for a specified duration. Once the sample had been damaged in this manner, the hole depth was measured for a given location, thus determining the hole depth evolution as a function of time. It is not feasible to develop pictures analogous to Figure 5, however, the hole depth as a function of time for the experiment are presented in Figure 7:

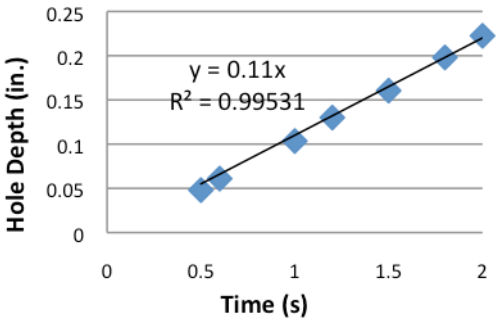


**Figure 7**. Experimental Hole Depth vs. Time

Figure 7 also suggests that the hole depth evolves approximately linearly with respect to time. The hole can be seen to progress at a rate of approximately 0.11in/s. At the end of the experiment, the hole diameter on the laser impact side was measured to be 0.298in.

## 6. Conclusions

Beginning with the COMSOL transient heat transfer module, we have developed a working model for the evolution of a laser induced hole in an isotropic polymeric material. To accomplish this, we have included conduction, convection, and radiation heat transfer. The model also makes allowances for the absorbed energy of phase transformation, material removal, and transition of energy application from the system boundary to the pit surface.

The simulation predicts a hole evolution rate of 0.136in/s. The experimental results demonstrate a hole evolution rate of 0.11in/s; a theoretical over-prediction of 20%. The theoretically predicted hole diameter compares favorably to within 2.2%. In summary, the model developed here has been demonstrated to be a fairly good predictive tool for the evolution of damage from a high energy laser provided one has complete knowledge of the materials being impacted.

## 7. References


1. Robert Cozzens, Infrared Laser Ablation of Polymers, *Polymer Engineering and Science,* **18**, 1978.
2. Christopher Lloyd, Ablative Polymeric Materials for Near Infrared High-Energy Laser Beam Diagnostics, *Journal of Directed Energy*, **3**, 2009.
3. KCA Crane, Laser-Induced Ablation of Fibre/Epoxy Composites, *Journal of Applied Physics,* **14,** 1981.
4. KT Voisey, Fibre Swelling During Laser Drilling of Carbon Fiber Composites, *Optics and Lasers in Engineering,* **44,** 2006.
5. CT Pan, Evaluation of Anisotropic Thermal Conductivity for Unidirectional FRP in laser Machining, *Composites Part A*, **32**, 2001.
6. CT Pan, Prediction of Extent of HAZ in Laser Grooving of Unidirectional Fiber Reinforced Plastics, *Journal of Engineering Materials and Technology,* **120**, 1998.
7. E Uhlmann, The Extent of Laser Induced Thermal Damage of UD and Crossply Composite Laminates, *International Journal of Machine Tools & Manufacture*, **39**, 1999.
8. WSO Rodden, A Comprehensive Study of the Long Pulse Nd:YAG Laser Drilling of Multi-Layer Carbon Fiber Composites, *Optics Communications,* **210,** 2002.
9. MD Islam, Thermal Conductivity of Fiber Reinforced Composites by the FEM, *Journal of Composite Materials*, **33,** 1999.
10. CF Cheng, Application of a 3-D Heat Flow Model to Treat Laser Drilling of Carbon Fiber Composites, *Acta Metallurgica,* 1998.
11. LN Nikitin, Calculation of the Temperature of Polymer or Composite Surfaces Placed in an Infrared Laser Field, *Mechanics of Composite Materials*, **31**, 1995.
12. Toshiki Hirogaki, Prediction of Damage Width in Laser Drilling of Printed Wiring Board using FEM, *ICCM Proceedings*, 1997.
13. Robert Cozzens, High Energy Laser Interactions with Organic Matrix Composites, *Naval Research Laboratory*, 2007. (FOUO)
14. Solid State laser Technology Maturation program WAREX, *ONR*, 2012. (Distribution F).
15. Christopher Lloyd, Ablative Polymeric Materials for Near-Infrared High-Energy Laser Beam Diagnostics, *Journal of Directed Energy*, **3,** 2009.
16. Christopher Lloyd, Near Infrared Laser Ablation of Organic Polymeric Materials, Doctoral Thesis, 2009.
17. M Dell'erba, An Experimental Study on Laser Drilling and Cutting of Composite

Materials for the Aerospace Industry Using Excimer and CO2 Sources, *Composites Manufacturing*, **3**, 1992.
18. Barbara Garrison, Laser Ablation of Organic Polymers: Microscopic Models for Photochemical and Thermal Processes, *Journal of Applied Physics*, **57**, 1985.
19. CF Cheng, Application of a Three Dimensional Heat Flow Model to Treat Laser Drilling of Carbon Fiber Composites, *Acta Metallurgica*, **46,** 1998.
20. D Groulx and W Ogoh, Solid-Liquid Phase Change Simulation Applied to a Cylindrical Latent Heat Energy Storage System

## 8. Acknowledgements

The authors would like to thank the Dr. Quentin Salter, Research Program Officer, Office of Naval Research for his generous support of this research.

## 9. Appendix

Table 1: Model Material Properties

| Property | Symbol | Value |
|---|---|---|
| PMMA Density | $\rho_s$ | 1070 kg/m$^3$ |
| Air/Vapor Density | $\rho_v$ | 1 kg/m$^3$ |
| PMMA Thermal Conductivity | $k_s$ | 0.19 W/mK |
| PMMA Specific Heat | $C_{P,s}$ | 1470 J/kg-K |
| Air/Vapor Specific Heat | $C_{P,v}$ | 1000 J/kg-K |
| Latent Heat of Phase Change | $\Delta_h$ | 620 kJ/kg |
| Convection Coefficient | $h$ | 25W/m$^2$ |
| Emissivity | $\varepsilon$ | 0.85 |
| Phase Change End Temperature | $T_1$ | 310°C |
| Phase Change Start Temperature | $T_2$ | 475°C |
| Reflectivity | $R_{\%}$ | 0.45 |
| Laser Power | $P$ | 110W |
| Beam Diameter | $D$ | 5.454mm |
| Domain Radius | $R$ | 3in. |
| Domain Thickness | $H$ | 0.5in |